Adhesive Contact: Scale issues

E. Barthel[1], A. Perriot[1], G. Haiat[2], A. Chateauminois[3] and C. Frétigny[3]

[1]Surface du Verre et Interfaces, CNRS/Saint-Gobain

[2]B2OA, CNRS/Paris XI

[3]PPMD, CNRS/ESPCI.

2010

An adhesion problem

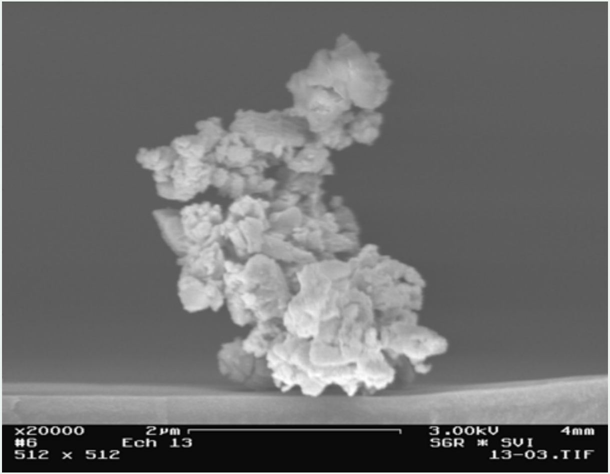

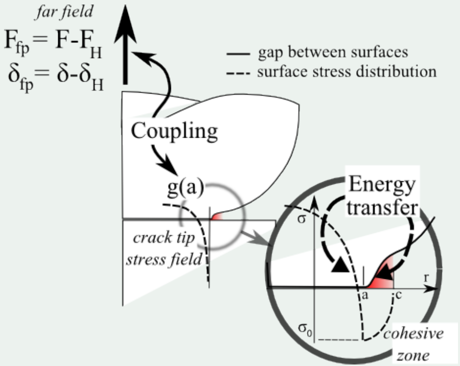

Figure: Coupling between far field an cohesive zone.

The standard case – Homogeneous elastic

- Adhesion energy – phenomenology of the contact
- Impact of surface interaction details

Non homogeneous systems

- Coatings – Experiments
- Coatings – Models

Time dependent – Viscoelastic materials

- Viscoelastic materials – Experiments
- Viscoelastic materials – Models

Outline

a	contact radius

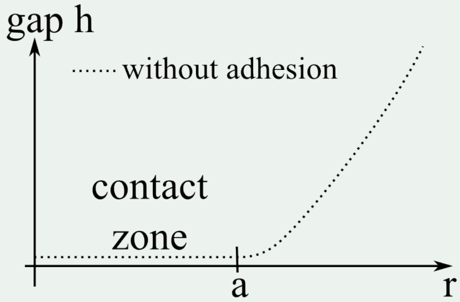

Figure: Hertz contact.

a	contact radius
w	adhesion energy

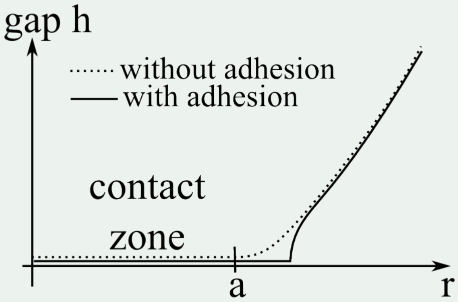

Figure: With adhesion.

a	contact radius
w	adhesion energy
δ_{fp}	flat punch disp.

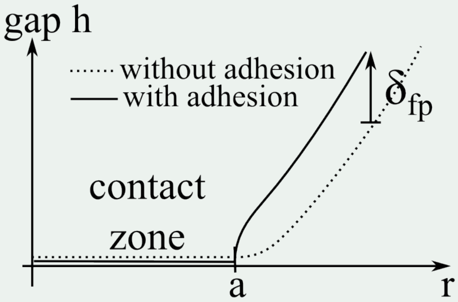

Figure: With adhesion at constant radius.

the flat punch displacement

$$E^* {\delta_{fp}}^2 = 2\pi a w$$

A hand waving argument

$$\mathcal{E} \simeq E^\star \left(\frac{\delta}{a}\right)^2 a^3$$

$$\frac{d\mathcal{E}}{d(\pi a^2)} = w$$

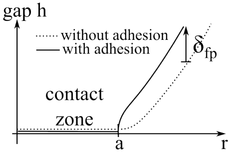

Figure: With adhesion at constant radius.

Force – flat punch contribution

$$F_{fp} = S(a)\delta_{fp}$$

where

$$S(a) = \frac{dF_{hertz}}{d\delta_{hertz}} = 2aE^{\star}$$

is the contact stiffness

a	contact radius
δ_{fp}	flat punch disp.
w	adhesion energy
E^*	reduced modulus
S(a)	contact stiffness

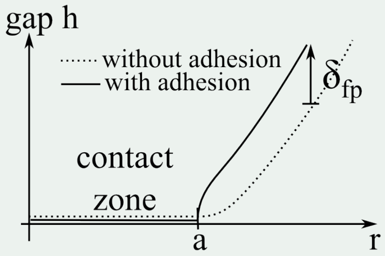

$$\delta = \delta_H + \delta_{fp}$$
$$F = F_H + F_{fp}$$

with

$$F_{fp} = S(a)\delta_{fp}$$

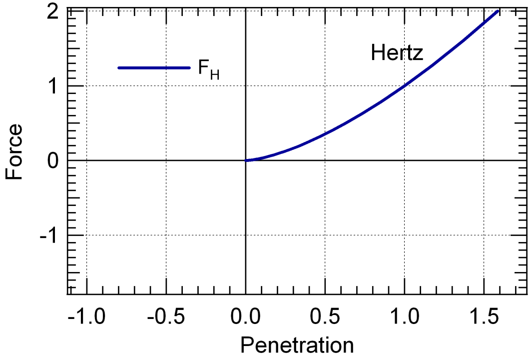

Figure: Hertz contact.

$$\delta = \delta_H + \delta_{fp}$$
$$F = F_H + F_{fp}$$

with

$$F_{fp} = S(a)\delta_{fp}$$

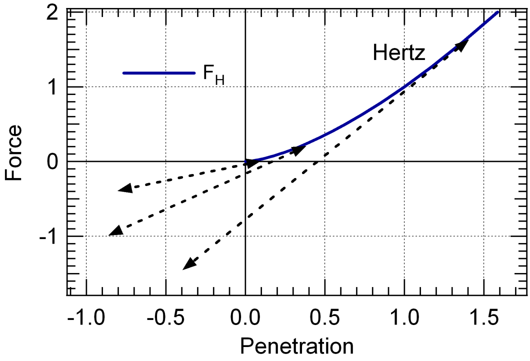

Figure: With flat punch contribution.

$$\delta = \delta_H + \delta_{fp}$$
$$F = F_H + F_{fp}$$

with

$$F_{fp} = S(a)\delta_{fp}$$

and

$$E^*{\delta_{fp}}^2 = 2\pi a w$$

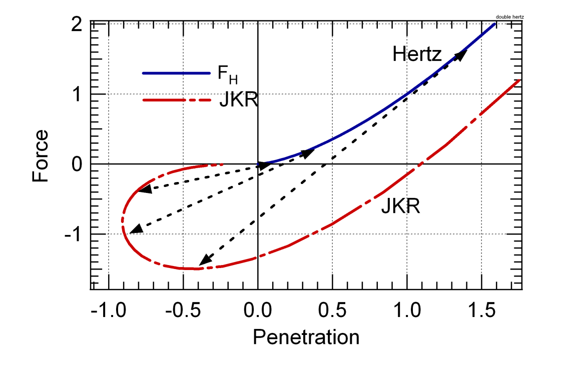

Figure: JKR adhesive contact.

JKR equations

For a sphere of radius R

$$\delta_{JKR} = \frac{a^2}{R} - \sqrt{\frac{2\pi a w}{E^\star}}$$

$$F_{JKR} = \frac{4E^\star a^3}{3R} - 2\sqrt{2\pi a^3 w E^\star}$$

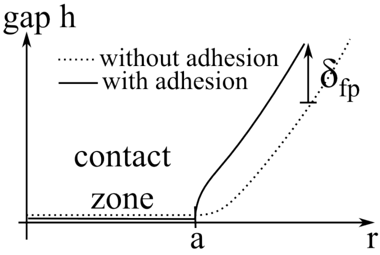

Figure: With adhesion at constant radius.

[Johnson 1971]

Orders of magnitude at rupture

$$F_{adh} = \frac{3}{2}\pi R w$$

$$\delta_{fp} = \left(\frac{\pi w^2 R}{E^{\star 2}}\right)^{1/3}$$

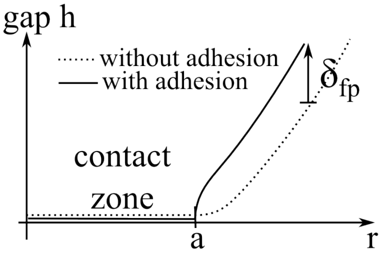

Figure: With adhesion at constant radius.

[Johnson 1971]

Does it conform to our experience ?

1. gravity against surface forces
2. surface forces win if

$$R^2 < w/\rho g$$

3. Cut-off radius around 1 mm !!!

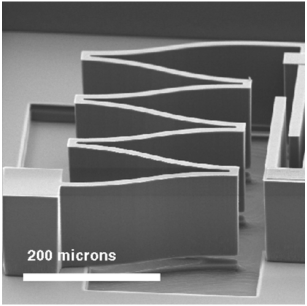

Figure: A typical MEMS

There is something more to it...roughness

SAINT-GOBAIN cnrs

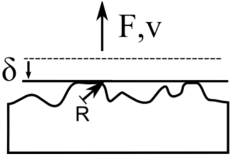

Figure: Meniscus mediated adhesive contact.

For $R \simeq 1\ \mu$m and
$E^\star \simeq 1$ MPa,
$\delta_f p \simeq 0.3\ \mu$m.

From [Fuller 1975]

Impact of roughness

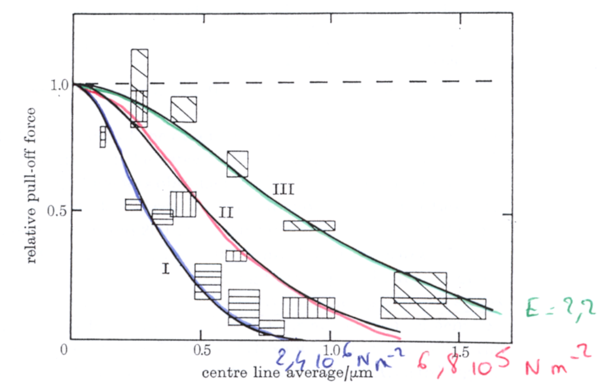

Figure: Impact of roughness as a function of modulus.

Outline

SAINT-GOBAIN

cnrs
dépasser les frontières

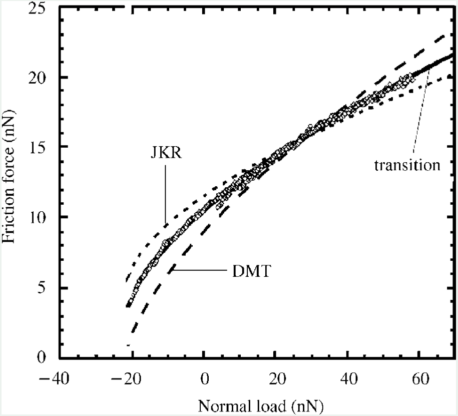

Figure: JKR does not explain all.

From [Grierson 2005]

Surface interactions

Interaction potential $V(z)$
Cohesive stresses

$$\sigma_{coh} = -\frac{dV}{dz}$$

and adhesion energy

$$w = V(+\infty) - V(0)$$

so that

$$w = -\int_0^{+\infty} \sigma_{coh}(z)\ dz$$

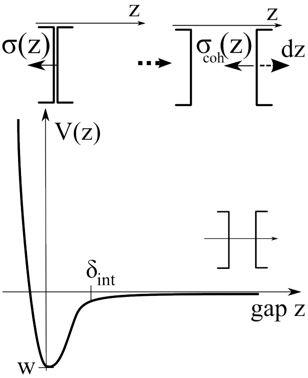

Figure: Interaction energy as a function of surface separation

Can we measure the cohesive stresses directly ?

1. Surface forces measurements with fine tips allow for direct measurement of local inter-surface interactions
2. note long range contribution

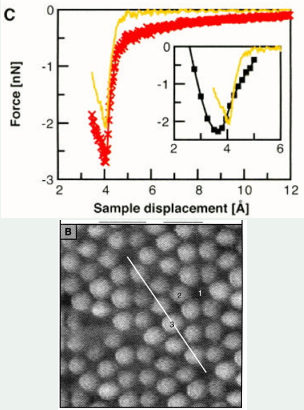

Figure: Tip/surface interaction.

After [Lantz 2001]

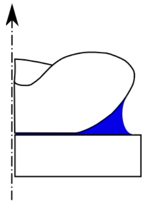

Figure: Meniscus mediated adhesive contact.

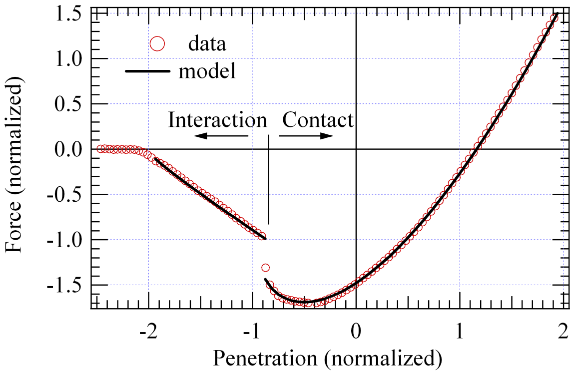

Figure: Meniscus mediated surface forces.

From [Barthel 1996]

Self-consistence

$$w = -\int_a^{+\infty} \sigma_{coh}(r) \frac{\partial h}{\partial r} dr$$

with the gap

$$h = h_{coh} + h_{hertz}$$

so that

$$w = \alpha \frac{{\sigma_{coh}}^2 \epsilon}{E^\star} + \beta(a)\sigma_{coh}$$

Cohesive zone

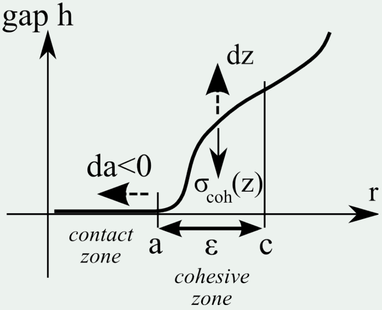

Figure: Cohesive zone.

Self-consistence

$$w = \frac{\pi}{4}\frac{{\sigma_{coh}}^2\epsilon}{E^\star} + \beta(a)\sigma_{coh}$$

Local deformation contribution

$$w = \frac{g(a)^2}{\pi a}\frac{2}{E^\star}$$

"pseudo" stress intensity factor

$$g(a) = \frac{\pi\sqrt{a}}{2\sqrt{2}}\,\sigma_{coh}\sqrt{\epsilon}$$

Coupling to the far field

Macroscopic calculation of local deformation effects

$$w = \frac{E^\star \delta_{fp}^2}{2\pi a}$$

Coupling

$$\delta_{fp} = \frac{2}{E^\star} g(a)$$

Self-consistence

$$w = \frac{\pi}{4}\frac{{\sigma_{coh}}^2\epsilon}{E^\star} + \beta(a)\sigma_{coh}$$

Local deformation contribution

$$w = \frac{g(a)^2}{\pi a}\frac{2}{E^\star}$$

"pseudo" stress intensity factor

$$g(a) = \frac{\pi\sqrt{a}}{2\sqrt{2}}\,\sigma_{coh}\sqrt{\epsilon}$$

Coupling to the far field

Macroscopic calculation of local deformation effects

$$w = \frac{E^\star\delta_{fp}^2}{2\pi a}$$

Coupling

$$\delta_{fp} = \frac{2}{E^\star}g(a)$$

Self-consistence

$$w = \frac{\pi}{4}\frac{{\sigma_{coh}}^2\epsilon}{E^\star} + \beta(a)\sigma_{coh}$$

Local deformation contribution

$$w = \frac{g(a)^2}{\pi a}\frac{2}{E^\star}$$

"pseudo" stress intensity factor

$$g(a) = \frac{\pi\sqrt{a}}{2\sqrt{2}}\,\sigma_{coh}\sqrt{\epsilon}$$

Coupling to the far field

Macroscopic calculation of local deformation effects

$$w = \frac{E^\star\delta_{fp}^2}{2\pi a}$$

Coupling

$$\delta_{fp} = \frac{2}{E^\star}g(a)$$

Self-consistence

$$w = \frac{\pi}{4} \frac{{\sigma_{coh}}^2 \epsilon}{E^\star} + \beta(a)\sigma_{coh}$$

Local deformation contribution

$$w = \frac{g(a)^2}{\pi a} \frac{2}{E^\star}$$

"pseudo" stress intensity factor

$$g(a) = \frac{\pi\sqrt{a}}{2\sqrt{2}} \sigma_{coh}\sqrt{\epsilon}$$

Coupling to the far field

Macroscopic calculation of local deformation effects

$$w = \frac{E^\star \delta_{fp}^2}{2\pi a}$$

Coupling

$$\delta_{fp} = \frac{2}{E^\star} g(a)$$

Self-consistence

$$w = \frac{\pi}{4}\frac{{\sigma_{coh}}^2\epsilon}{E^\star} + \beta(a)\sigma_{coh}$$

Local deformation contribution

$$w = \frac{g(a)^2}{\pi a}\frac{2}{E^\star}$$

"pseudo" stress intensity factor

$$g(a) = \frac{\pi\sqrt{a}}{2\sqrt{2}}\,\sigma_{coh}\sqrt{\epsilon}$$

Coupling to the far field

Macroscopic calculation of local deformation effects

$$w = \frac{E^\star\delta_{fp}^2}{2\pi a}$$

Coupling

$$\delta_{fp} = \frac{2}{E^\star}g(a)$$

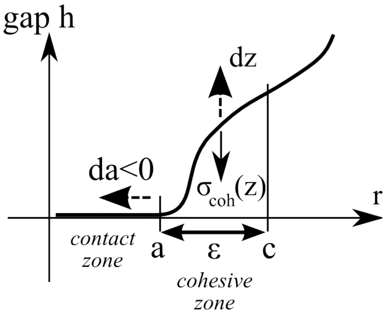

Figure: Cohesive zone.

Macroscopic relations

$$\delta = \delta_H + \delta_{fp}$$
$$F = F_H + F_{fp} + F_{ext}$$

Ref: [Barthel 2008]

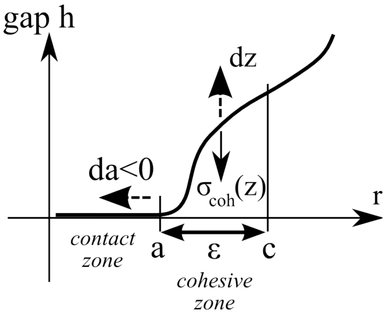

Figure: Cohesive zone.

Macroscopic relations

$$
\begin{aligned}
\delta &= \delta_H + \delta_{fp} \\
F &= F_H + F_{fp} + F_{ext}
\end{aligned}
$$

Ref: [Barthel 2008]

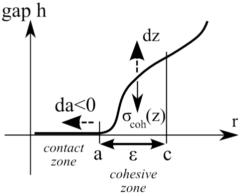

Figure: Cohesive zone.

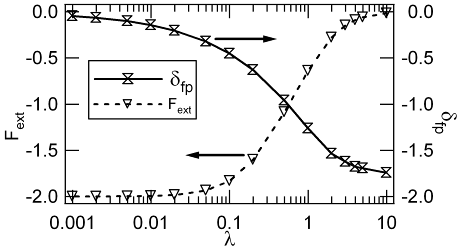

Figure: Cohesive zone and flat punch contributions.

$$\lambda \equiv \frac{\delta_{fp}}{\delta_{int}} \simeq \frac{\delta_{fp}\sigma_{coh}}{w} = \frac{\sigma_{coh}}{\left(\frac{wE^{\star 2}}{\pi R}\right)^{1/3}}$$

Ref: [Tabor 1977, Maugis 1992]

The lower lengthscale problem

Animal pad division

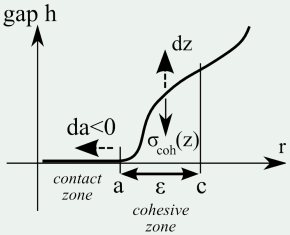

Average stress

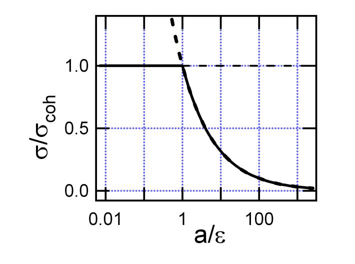

Figure: Cut-off with size reduction.

After [Arzt 2003]

The lower lengthscale problem

Animal pad division

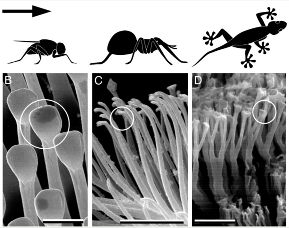

Figure: Various pads as a function of species.

Size Effect

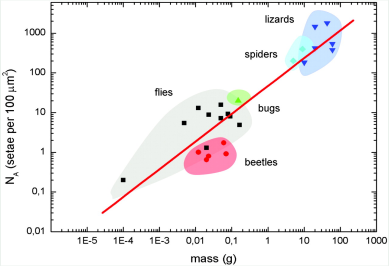

Figure: Pad division as a function of weight.

After [Arzt 2003]

Outline

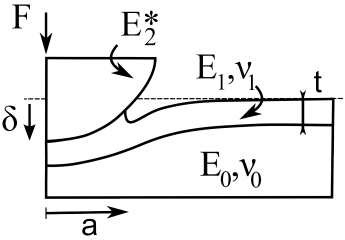

Figure: Adhesive contact in the presence of a thin film.

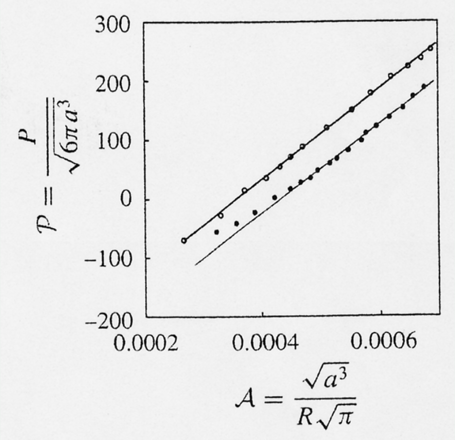

Figure: Force vs contact radius.

From [Tardivat 2001]

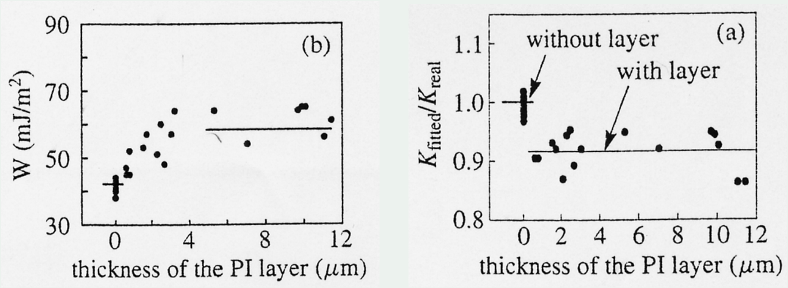

Figure: Effective adhesion energy and modulus as a function of film thickness.

From [Tardivat 2001]

$E^{\star}{}_2$	1.95 MPa
E_1	3.5 MPa

Outline

$$\delta(a,t,[E]) = \delta_H(a,t,[E]) + \delta_{fp}$$
$$F(a,t,[E]) = F_H(a,t,[E]) + S(a,t,[E])\delta_{fp}$$

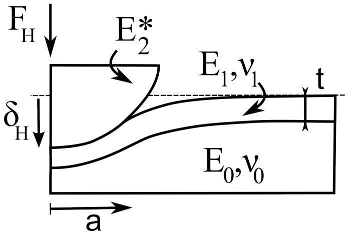

Figure: Adhesive contact in the presence of a thin film.

[Barthel 2007]

$$\delta(a,t,[E]) = \delta_H(a,t,[E]) + \delta_{fp}$$
$$F(a,t,[E]) = F_H(a,t,[E]) + S(a,t,[E])\delta_{fp}$$

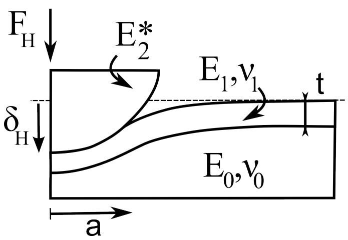

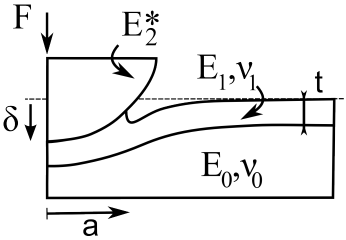

Figure: Adhesive contact in the presence of a thin film.

[Barthel 2007]

the flat punch displacement – Compliance method

$$\frac{1}{2}\delta_{fp}^2 \frac{dS}{da} = 2\pi a w$$

A hand waving argument

$$\mathcal{E} \simeq \frac{1}{2} S {\delta_{fp}}^2$$

and

$$\frac{d\mathcal{E}}{d(\pi a^2)} = \frac{1}{2}\frac{1}{2\pi a}\frac{dS}{da}$$

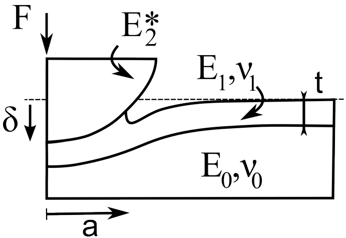

$E^{\star}{}_2$	1.95 MPa
E_1	3.5 MPa

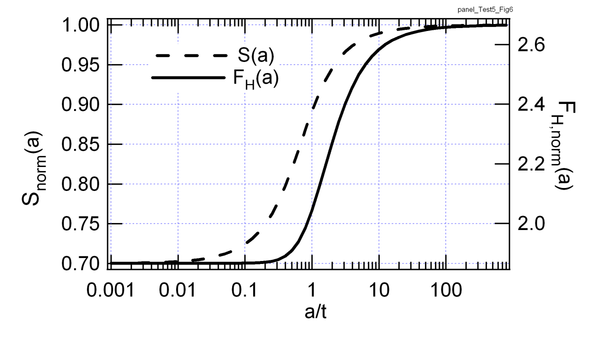

Figure: Effective stiffness and force as a function of film thickness.

See [Yu 1990, Schwarzer 1993, Perriot 2004, Sridhar 2004, Mary 2006]...

$$\eta = \frac{t}{\left(\frac{\pi w R^2}{E_1{}^\star}\right)^{1/3}}$$

$$\bar{a} = \eta \tilde{a}$$

$$D_s = (\eta\tilde{a})^2 \, \Delta_{s,0} - \sqrt{2}\,(\eta\tilde{a})^{1/2} \, \frac{1}{\Gamma(1)}$$

$$\Pi_s = (\eta\tilde{a})^3 \, \frac{\Pi_{s,0}}{2} - 2\sqrt{2}\,(\eta\tilde{a})^{3/2} \, \frac{\mathcal{E}_{eq}}{\Gamma(1)}$$

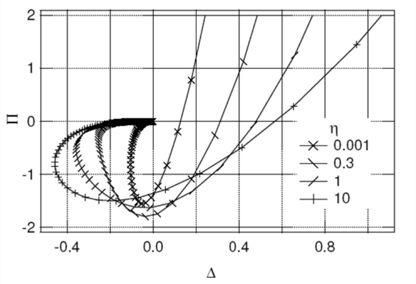

Figure: Force vs. penetration fr a coated substrate.

[Barthel 2007]

SAINT-GOBAIN

CNRS

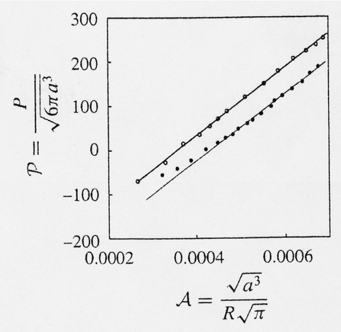

Figure: Force vs contact radius.

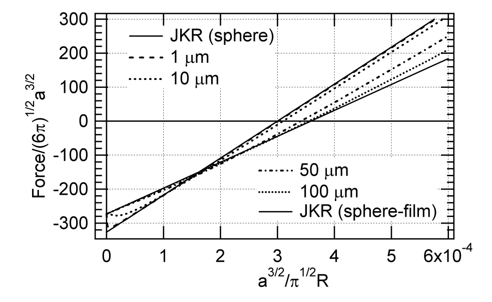

Figure: Adhesion force vs. contact radius.

[Tardivat 2001, Barthel 2007]

$E^\star{}_2$	1.95 MPa
E_1	3.5 MPa

SAINT-GOBAIN cnrs

Outline

elastomeric contact

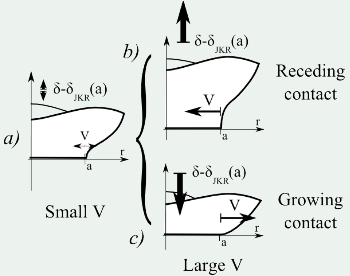

Figure: Receding and growing contacts for a viscoelastic material.

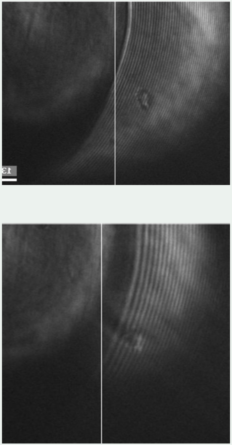

Charrault 2009.

SAINT-GOBAIN

cnrs

Growing contact

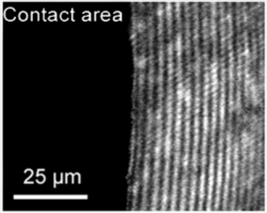

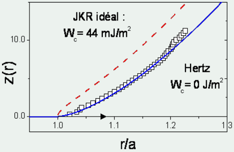

Receding contact

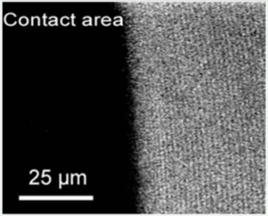

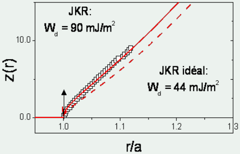

C. Gauthier et al.

SAINT-GOBAIN cnrs

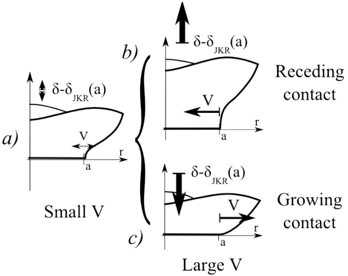

Figure: Growing and receding contacts for a viscoelastic material.

Typical JKR data

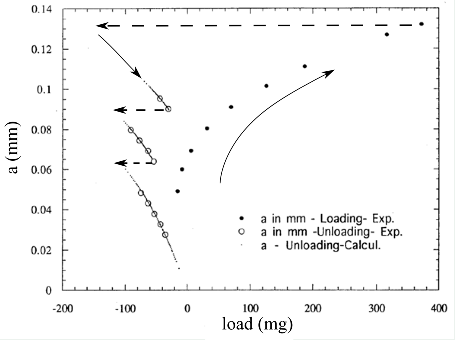

Figure: Force vs contact radius for the adhesive contact of an elastomer.

From [Deruelle 1995]

Outline

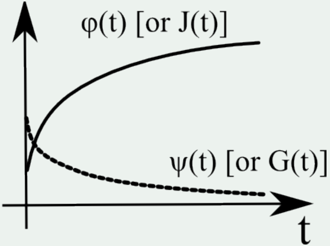

Figure: Creep and relaxation functions for a viscoelastic material.

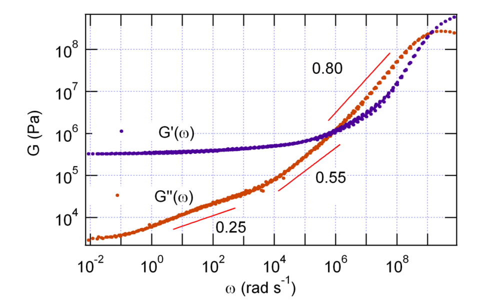

Figure: Real and imaginary parts of the modulus of natural rubber.

$$\phi(0) = \frac{2}{E^\star(t=0)},\ \phi(\infty) = \frac{2}{E^\star(t=\infty)}$$
$$k = E^\star(t=\infty)/E^\star(t=0) \ll 1$$

Data H. Montes, PPMD.

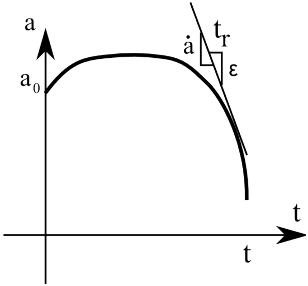

Figure: History of contact radius for a viscoelastic material.

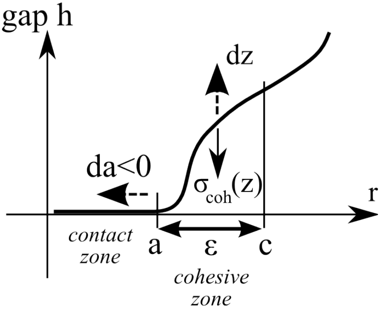

Figure: Cohesive zone.

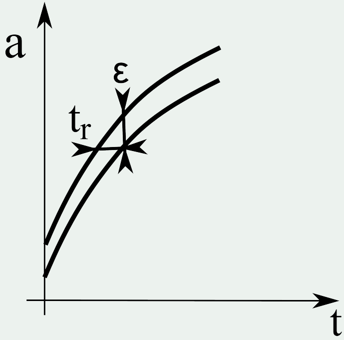

Figure: Convected cohesive zone.

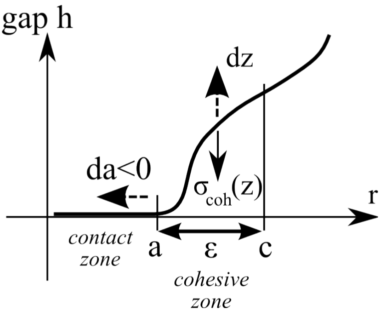

Figure: Cohesive zone.

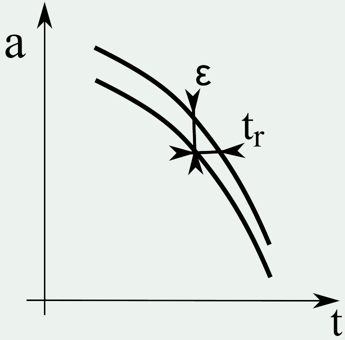

Figure: Convected cohesive zone.

Effective modulus of cohesive zone

$$w = \frac{g(a)^2}{\pi a}\phi_1(t_r)$$

with

$$\phi_{1,cl}(t) = \frac{2}{t^2}\int_0^t \tau\phi(\tau)d\tau \quad \text{(closing)}$$

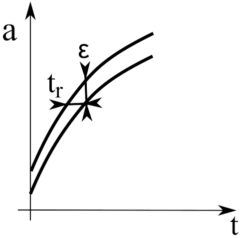

Figure: Convected cohesive zone.

From [Barthel 2008]

Effective modulus of cohesive zone

$$w = \frac{g(a)^2}{\pi a}\phi_1(t_r)$$

with

$$\phi_{1,op}(t) = \frac{2}{t^2}\int_0^t (t-\tau)\phi(\tau)d\tau \quad \text{(opening)}$$

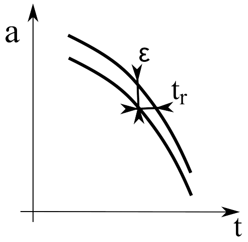

Figure: Convected cohesive zone.

From [Barthel 2008]

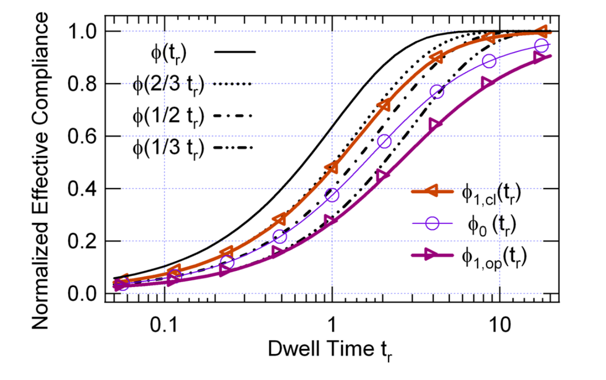

Figure: Effective compliances.

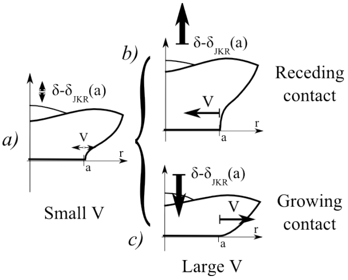

Figure: Growing and receding contacts for a viscoelastic material.

From [Barthel 2008]

Effective coupling constant

- Receding contact

$$\delta_{fp} \simeq \phi_0(\infty) g(a) = \frac{2}{E^\star(\infty)} g(a)$$

- Growing contact

$$\delta_{fp} \simeq \phi_0(t_r) g(a)$$

where

$$\phi_0(t) = \frac{1}{t} \int_0^t d\tau \phi(t-\tau)$$

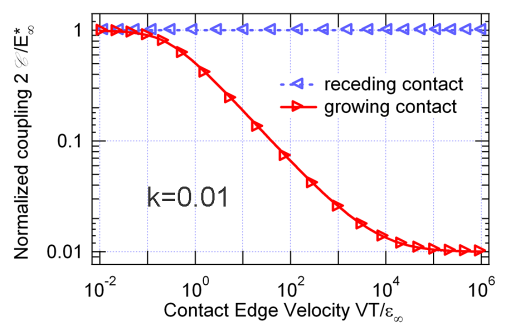

Figure: Coupling constants.

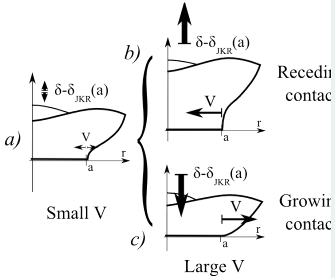

Figure: Far field and adhesion of elastomers.

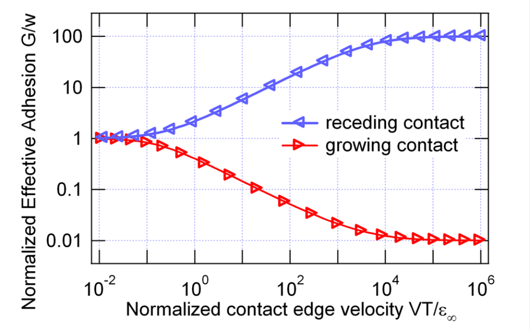

Figure: Effective adhesion.

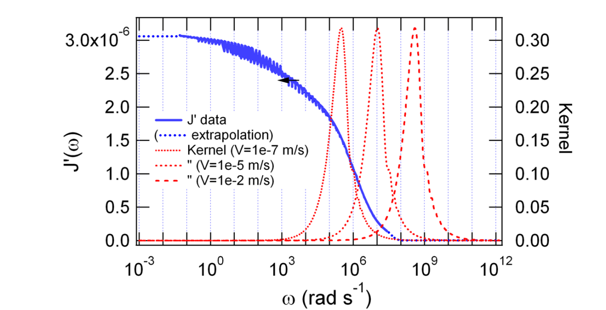

Figure: Effective adhesion from compliance.

Barthel and Fretigny, to be publ.

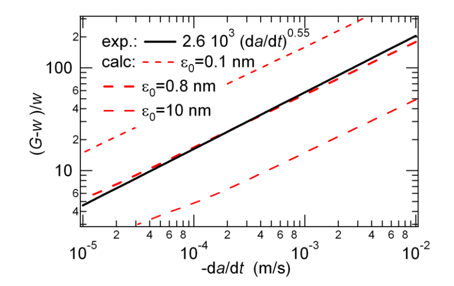

Figure: Calculated effective toughness.

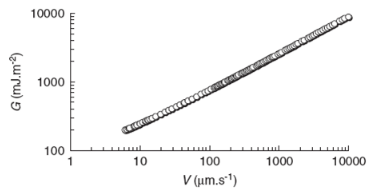

Figure: Toughness data.

[Tay 2006]

Conclusion

- macroscopic description
  energy balance
- details of surface interactions
  cohesive stresses – self consistent description
- coatings
  macroscopic description – compliance method
- time dependent materials
  cohesive stresses couple to dissipative material response

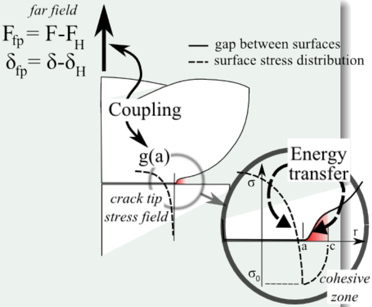

Figure: Coupling between far field an cohesive zone.

E. Arzt, S. Gorb, and R. Spolenak.
From micro to nano contacts in biological attachment devices.
Proc. Natl. Acad. Sci. USA, 100(19):8 – 10, 2003.

E. Barthel.
Elastic adhesive contact – JKR and more.
J. Phys. D: Appl. Phys., 41:163001, 2008.

E. Barthel, X. Y. Lin, and J. L. Loubet.
Adhesion energy measurements in the presence of adsorbed liquid using a rigid surface force apparatus.
J. Colloid Interface Sci., 177:401–406, 1996.

E. Barthel and A. Perriot.
Adhesive contact to a coated elastic substrate.
Journal of physics D: Applied physics, 40:1059–1067, 2007.

M. Deruelle, L. Leger, and M. Tirrel.
Adhesion at the solid-elastomer interface : influence of the interfacial chains.

Macromolecules, 28:7419–7428, 1995.

K. Fuller and D. Tabor.
The effect of surface roughness on the adhesion of elastic solids.
Proc. Roy. Soc. A, 345:327–342, 1975.

D. S. Grierson, E. E. Flater, and R. W. Carpick.
Accounting for the JKR-DMT transition in adhesion and friction measurements with atomic force microscopy.
J. Adhesion Sci. Technol., 19:291–311, 2005.

K. L. Johnson, K. Kendall, and A. D. Roberts.
Surface energy and the contact of elastic solids.
Proc. Roy. Soc. London A, 324:301–313, 1971.

M. A. Lantz, H. J. Hug, R. Hoffmann, P. J. A. Van Schendel, P. Kappenberger, S. Martin, A. Baratoff, and H.-J. Güntherodt.

Quantitative measurement of short-range chemical bonding forces.
Science, 291:2580–2583, 2001.

P. Mary, Chateauminois A., and C. Fretigny.
Deformation of elastic coatings in adhesive contacts with spherical probes.
Journal-of-Physics-D-Applied-Physics, 39:3665–73, 2006.

D. Maugis.
Adhesion of spheres: The JKR-DMT transition using a dugdale model.
J. Colloid Interface Sci, 150:243–69, 1992.

A. Perriot and E. Barthel.
Elastic contact to a coated half-space: Effective elastic modulus and real penetration.
J. Mater. Res., 19:600–608, 2004.

N. Schwarzer, F. Richter, and F. Hecht.

Determination of mechanical properties of thin films : a theoretical feasibility study.
Surface and coatings technology, 60:396–400, 1993.

I. Sridhar, Z. W. Zheng, and K. L. Johnson.
A detailed analysis of adhesion mechanics between a compliant elastic coating and a spherical probe.
J. Phys. D: Appl. Phys., 37:2886–2895, 2004.

D. Tabor.
Surface forces and surface interactions.
J. Colloids Interface Sci., 58:2, 1977.

C. Tardivat, H. Hervet, and L. Léger.
Adhesion evaluation for a stratified system in jkr geometry.
J. Adhes. Sci. Technol., 15:1055–1078, 2001.

A. Tay and M. Barquins.
Detachment of glass balls from smooth rubber under gravity.
Int. J. Adhes. Adhes., 26:371–377, 2006.

H. Y. Yu, S. C. Sanday, and B. B. Rath.
The effect of substrate on the elastic properties of films determined by the indentation test : axisymmetric boussinesq problem.
J. Mech. Phys. Sol., 38:745–764, 1990.